

RSC Advances



This is an *Accepted Manuscript*, which has been through the Royal Society of Chemistry peer review process and has been accepted for publication.

Accepted Manuscripts are published online shortly after acceptance, before technical editing, formatting and proof reading. Using this free service, authors can make their results available to the community, in citable form, before we publish the edited article. This *Accepted Manuscript* will be replaced by the edited, formatted and paginated article as soon as this is available.

You can find more information about *Accepted Manuscripts* in the [Information for Authors](#).

Please note that technical editing may introduce minor changes to the text and/or graphics, which may alter content. The journal's standard [Terms & Conditions](#) and the [Ethical guidelines](#) still apply. In no event shall the Royal Society of Chemistry be held responsible for any errors or omissions in this *Accepted Manuscript* or any consequences arising from the use of any information it contains.

Cite this: DOI: 10.1039/c0xx00000x

www.rsc.org/xxxxxx

ARTICLE TYPE

Porous reduced graphene oxide wrapped carbon nanotube-manganese dioxide nanocables with enhanced electrochemical capacitive performance

Yiran Kang,^{a,b} Feng Cai,^{a,c} Hongyuan Chen,^a Minghai Chen,^{a,*} Rui Zhang,^{b,d} and Qingwen Li^{a,*}*Received (in XXX, XXX) Xth XXXXXXXXX 20XX, Accepted Xth XXXXXXXXX 20XX*

DOI: 10.1039/b000000x

MnO₂ has ultra-low conductivity for electrodes of supercapacitors. In this research, porous reduced graphene oxide (rGO) wraps on MnO₂ nanoflowers with a conductive carbon nanotube core (CNT-MnO₂). This nanostructure could effectively improve the surface and inner conductivity of the composites. Unlike pristine rGO, the porous rGO does not block the diffusion of electrolyte into the inner part of the composites, which allows the utilization of MnO₂ in this composite capacitor very well. As a result, the as-prepared CNT-MnO₂-porous rGO ternary hybrid material shows superior specific capacitance and rate performance to pristine CNT-MnO₂ nanocables and pristine rGO wrapped CNT-MnO₂ nanocables. This synthesis strategy could be valuable for the design of better performance pseudocapacitive electrodes for supercapacitors.

1. Introduction

Nowadays, the development of new energy storage devices with high energy/power densities has attracted much attention for the gradual short of traditional fossil energy and the aggravating trend of global warming. Among these devices, electrochemical supercapacitor has occupied an important position for its superior performance such as high power density,¹⁻⁴ long cycle lifetime, safety, operability and environmental friendly property.⁵⁻⁷ In general, electrode materials for supercapacitors could be classified into two types based on the charge/discharge mechanisms: electrical double layer capacitance materials (EDLC, mainly are carbon materials) and pseudocapacitive materials (including conducting polymers, metal oxides or hydroxides etc.). The former have high power density and excellent cyclic performance, but their energy density could not match the increase requirement of supercapacitors. As a result, the pseudocapacitance materials are more valuable for advanced supercapacitors.⁸

Among various pseudocapacitive electrode materials, manganese dioxide (MnO₂) has attracted much attention for its large operation voltage (~0.8 V, higher than Ni/Co hydroxide/oxide^{9,10}), low cost and environmental friendliness.¹¹ However, it suffers from inherent drawbacks for its low electrical conductivity (10⁻⁵-10⁻⁶ S cm⁻¹) and crystal shrinkage/expansion induced flaking off during charge/discharge cyclic process, which results in its low practical specific capacitance, poor rate performance and short cyclic lifetime.¹² Wrapping MnO₂ onto a conductive network could overcome these shortages to some extent. Carbon nanomaterials have excellent conductivity, supply high specific surface area to load active materials and especially

have good elasticity to accommodate the strain of volume change. One-dimensional carbon nanotube (CNT) owns outstanding electrical conductivity in its axis direction, thus could serve as a unique charge transfer channel in the electrode.¹³ Hierarchical MnO₂ nanostructures could grow onto individual CNT by different strategies, such as redox reaction^{14,15} and electrodeposition¹⁶. These nanostructures usually have large specific area for increasing electrochemical reaction area, thus utilizing MnO₂ as electrochemical active materials. Furthermore, the CNT core could ensure the inner conductivity of the hybrid structure. However, the surface conductivity of MnO₂ nanostructure is not improved. The practical performance of MnO₂ electrode is still limited by the low electron transfer rate and the difficulty forming stable electrochemical double layer (EDL) on the surface of MnO₂. Consequently, if a conducting layer can wrap around them, this problem can be effectively resolved. Single-walled CNT¹⁷ and conductive polymers¹⁸ have already been tried to be used as the conductive layer on MnO₂ surface, and the results shows improved performance. However, CNT wrapping could not achieve large coating area, and conductive polymer suffered from its low conductivity.¹⁹ Recently, reduced graphene oxide (rGO) has been regarded as an ideal conductive layer for the electrodes of lithium-ion batteries, because it has high conductivity and excellent Li-ion permeation performance.²⁰⁻²² Its coating onto the surface of electrode materials could effectively form EDL and enhance the surface conductivity of the electrodes. RGO coating strategy has already shown effective for enhancing the electrochemical performance of Li-ion battery electrodes. However, as the electrode of supercapacitors in aqueous electrolyte, the redox reaction of MnO₂ with electrolyte is largely relied to the contact between electrolyte and MnO₂. RGO coating layer could obstruct MnO₂

contact with electrolyte,²³ thus the material utilization efficiency and practical capacitance of MnO₂ could be limited. It is still a challenge to achieve both the enhancement of surface conductivity and high capacitance of MnO₂ electrode in supercapacitors.

In this paper, porous rGO was introduced as the conductive coating layer of CNT-MnO₂ hybrid nanocables to enhance the electrochemical performance of MnO₂ electrode for supercapacitors. Porous-rGO could both enhance the surface conductivity of MnO₂ and ensure the contact between electrolyte and MnO₂. As a result, the CNT-MnO₂-porous rGO ternary electrode showed superior specific capacitance and rate performance to pristine CNT-MnO₂ and CNT-MnO₂-rGO. Its specific capacitance could keep 71% at the current density from 100 mA·g⁻¹ to 2000 mA·g⁻¹, much better than pristine CNT-MnO₂ nanocables (51% retained) and CNT-MnO₂-rGO (53% retained). This novel structure and its assembling strategy could be valuable for the design of better performance electrodes for advanced supercapacitors.

2. Experimental Section

Materials. Graphene oxide (GO) was purchased from Tianjing Plannano Technology Co., Ltd, P. R. China. Carboxylated CNT was purchased from Chengdu Organic Chemicals Co. Ltd., Chinese Academy of Sciences. 20% poly (diallyldimethylammoniumchloride) (PDDA) (MW 100,000-200,000 g·mol⁻¹) and hydrazine hydrate (35 wt %) aqueous solution were purchased from Aldrich. NH₃·H₂O (25-28 wt %) and HNO₃ (68%) solution were obtained from Sino Pharm Chemical Reagent.

Synthesis. MnO₂ was deposited onto individual CNT through a direct redox reaction between the CNT and MnO₄⁻. Typically, 250 mg CNT powder was dispersed into 25 mL water with the assistance of ultrasonic treatment under the power of 300 W for 0.5 h. 0.1 M KMnO₄ aqueous solution of 50 mL was heated to 70 °C using a constant temperature water bath. Then, the as-prepared CNT dispersion was added into KMnO₄ solutions drop by drop and continuously magnetic stirred for 6 h. Finally, the mixture was centrifuged and washed with deionized water several times to remove the residual KMnO₄. The final product was CNT-MnO₂ nanocomposite. This as-prepared nanocomposite was dispersed in 250 mL water and mixed with 250 mL water containing 5 mL PDDA for 6h with the aim of functionalizing the powder by PDDA. After centrifuged and washed with deionized water for several times to remove the residual PDDA, 0.25 g CNT-MnO₂ powder was dispersed in 250 mL water again for further functionalization. Porous rGO was synthesized with the method mentioned in reference.²⁴ Firstly, pristine rGO was prepared by reducing 50 mL aqueous dispersion of GO (50 mg·mL⁻¹) with 50 μL hydrazine hydrate and 350 μL ammonia solution at 95 °C for 1 h. Then the dispersion was mixed with a certain amount of HNO₃ solution to form a mixture containing 8 mol L⁻¹ HNO₃ and then refluxed at 100 °C for 10 h. The mixture was centrifuged and washed with deionized water several times until the pH=7. Finally, they were dispersed in water to form a suspension with a typical concentration of 1 mg·mL⁻¹. To prepare the final ternary electrode material, 25 mL CNT-MnO₂-PDDA aqueous solution was mixed with 5 mL porous rGO and continuously magnetic stirred for 2 h. In the end, the mixture was

centrifuged and washed with deionized water for several times, and then dried at 70 °C for 12 h. The material assembling procedure and the schematic illustration of the ternary electrode was shown in Fig. 1.

Materials Characterization. The morphology of the samples was observed by field-emission scanning electron microscopy (FESEM, Quanta 400FEG, FEI) and transmission electron microscope (TEM, Tecnai G2 F20 S-Twin, FEI). The crystal structure of the products was examined by X-ray powder diffraction (XRD, D8Advance, 35 Bruker AXS). The Raman spectrum was measured by a laser confocal Raman microscopy (LabRAM HR, HORIBA Jobin Yvon). Zeta potential profiles of pristine rGO, porous rGO and CNT-MnO₂ nanocomposite before and after PDDA functionalization were measured at room temperature on a Malvern Instrument Nano-ZS Zeta potential analyzer.

Electrochemical Measurements. The electrochemical performance of the electrodes was measured by using CHI-660D electrochemical workstation in a three-electrode testing system at room temperature. 1 M Na₂SO₄ aqueous solution was used as electrolyte. A platinum wire was the counter electrode and a saturated calomel electrode (SCE) was the reference electrode. Cycling performance measurement of the sample was carried out on a Land battery testing system. The preparation of working electrodes was described as follows. Firstly, 4 mg of electrochemical active material powder were mixed with 0.75 mg acetylene black conductors and 0.15 mg polytetrafluoroethylene (PTFE) to form well-proportioned slurry. Then the obtained slurry was filled into a piece of nickel foam with an apparent area of 1 cm², and pressed under 10 MPa. Finally, the as-prepared electrode was heated at 70 °C for 12 h.

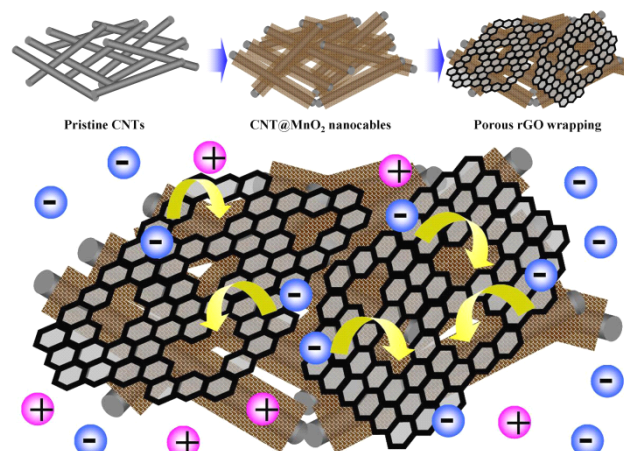


Fig. 1 Schematic illustration of the materials assembling process and the structure of CNT- MnO₂-porous rGO nanostructures.

3. Results and discussion

3.1. Characterization of CNT-MnO₂ nanocomposite

Fig. 2 shows the SEM images of pristine CNT and CNT-MnO₂ nanocomposite. It can be seen that the pristine CNT exhibits regular morphology with the diameter of about 30 nm as shown in Fig. 2a. After MnO₂ coating, CNT is converted to hierarchical nanowires with their diameter increasing to 90 nm (Fig. 2b and 2c), and the mass loading of MnO₂ can achieve about 92%

calculated from the TG curves shown in Fig. S1. MnO₂ nanosheets were uniformly coated onto the surface of individual CNT by the reaction between KMnO₄ and CNT. During the deposition process, the CNT acted as substrate and reducing agent for the reduction of MnO₄⁻ and the growth of MnO₂ nanoflakes.^{25,26} From the TEM image (Fig. 2d), it can be seen that the average size of the nanoflakes is about 30 nm and the thickness of the MnO₂ layer is about 30 nm.

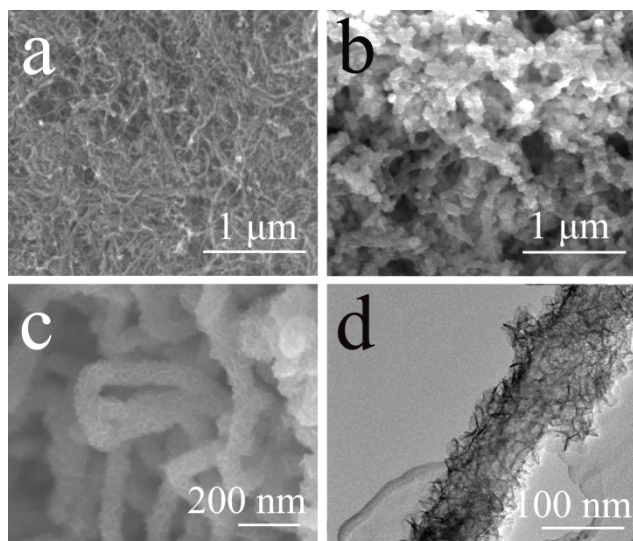


Fig. 2 SEM images of pristine CNT (a) and CNT- MnO₂ nanocables (b,c); TEM image of CNT- MnO₂ nanocables (d).

XRD patterns of CNT and CNT-MnO₂ nanocomposite are shown in Fig. 3a. The XRD pattern of pristine CNT shows three diffraction peaks at 26.5°, 43.2° and 54.2° which can be indexed as the (002), (100), and (004) reflections of graphite, respectively.²⁷ The three major diffraction peaks of 2θ at around 12°, 37° and 66° can be assigned to the crystal planes of (001), (111) and (020) in birnessite-type MnO₂ (JCPDS 42-1317, δ-MnO₂), respectively.²⁸⁻³¹ The weak and broad XRD peaks of MnO₂ mean that most MnO₂ is amorphous. This characteristic is beneficial for increasing the specific capacitance for the electrode, because the highly amorphous structure with abundant crystal defects should favor the electrolyte ion to diffuse into the oxide matrix, thus improving the utilization ratio of material.

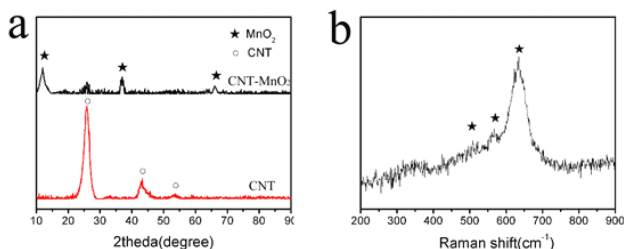


Fig. 3 XRD patterns of pristine CNT and CNT-MnO₂ nanocables (a); Raman spectrum of CNT-MnO₂ nanocables (b).

Raman spectrum is useful for analyzing the local structure of MnO₂, especially for samples with poor crystalline. The structural features of the CNT-MnO₂ nanocomposite were further

investigated using Raman measurements as shown in Fig. 3b. Three major features for MnO₂ can be recognized at 500, 575 and 640 cm⁻¹. The Raman band at 640 cm⁻¹ can be recognized as the symmetric stretching vibration (Mn-O) of the MnO₆ groups. The band located at 575 cm⁻¹ is usually attributed to the (Mn-O) stretching vibration in the basal plane of MnO₆ sheet.^{32,33} It indicates that the reaction product has the Raman spectra of the birnessite-type MnO₂.

3.2. Characterization of porous rGO and CNT-MnO₂-rGO/porous rGO nanocomposite

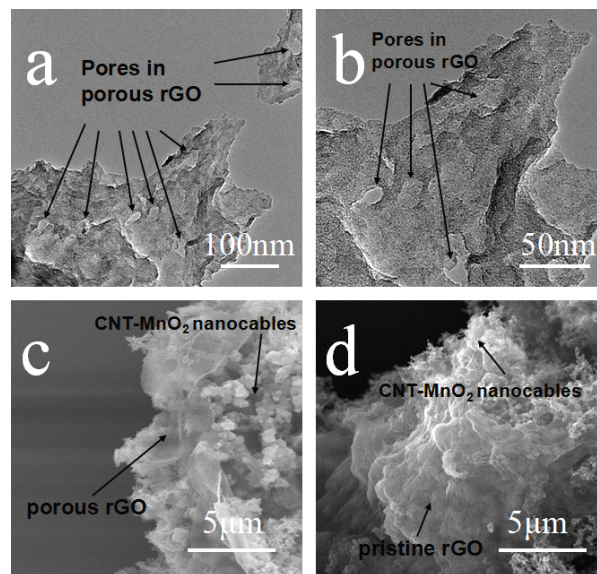


Fig. 4 TEM images of porous rGO (a,b) and SEM images of CNT-MnO₂-porous rGO (c) and CNT-MnO₂-non porous rGO nanostructures (d).

As shown in Fig. 4a and b, TEM images of porous rGO clearly show porous structure in a piece of rGO sheet. This is because nitric acid can selectively remove the defect clusters of pristine rGO sheets leaving pores in the basal planes of rGO sheets.²⁴ Figure. 4c and d show the morphology of CNT-MnO₂-porous rGO and CNT-MnO₂-rGO. The image in Fig. 4c indicates that CNT-MnO₂ nanocomposite was covered by porous rGO. Fig. 4d shows that CNT-MnO₂ nanocomposite could also be covered by pristine wrinkle rGO tightly. However, there is no obvious pore on this kind of rGO.

As is mentioned above, the surface charge of CNT-MnO₂ nanocomposite was modified by PDPA for the subsequent self-assembly of rGO and porous rGO on it, which was based on electrostatic attraction. The introduction of PDPA can change the surface charge of CNT-MnO₂ nanocomposite from electronegative status to electropositive status.³⁴⁻³⁶ After PDPA functionalization, the CNT-MnO₂ dispersion had a highly positive Zeta potential of 39.8 mV. Being compared with initial solution which had the Zeta potential of -40.2 mV, the surface charge of this modified solution had been changed obviously caused by the adsorption and coverage of PDPA on the external surface of CNT-MnO₂ nanocomposite.³⁷ The Zeta potentials of pristine rGO and porous rGO were tested to be -40.3 mV and -41.8 mV, due to the ionization of the partial oxygen functional groups that were not totally reduced. The Zeta potential results

above indicate that there exists a strong electrostatic attraction between the functional CNT-MnO₂ nanocomposites and pristine rGO/porous rGO nanosheets, which is the key to uniformly adsorption of rGO onto the surface of CNT-MnO₂ nanocomposite to prepare ternary electrode materials. As a result, when mixing the uniform dispersion of PDDA doped CNT-MnO₂ powder and porous rGO together, the ternary powder could be fast formed and deposited into the bottom of the bottle as shown in Fig.S2 in the electronic supplementary information. It indicated that the porous rGO could be effectively wrapped onto CNT-MnO₂ powder to form the ternary composite. As it mentioned before, the mass ratio between pristine CNT-MnO₂ powder and rGO or porous rGO was 5:1, and the content of CNT in the CNT-MnO₂ powder was 8% calculated according to the TG test. Thus in the final porous rGO wrapped CNT-MnO₂ composite, the content of MnO₂, CNT and porous rGO could be 76.66%, 6.67% and 16.67%, respectively.

3.3. Comparisons of the electrochemical capacitive performance of all electrodes

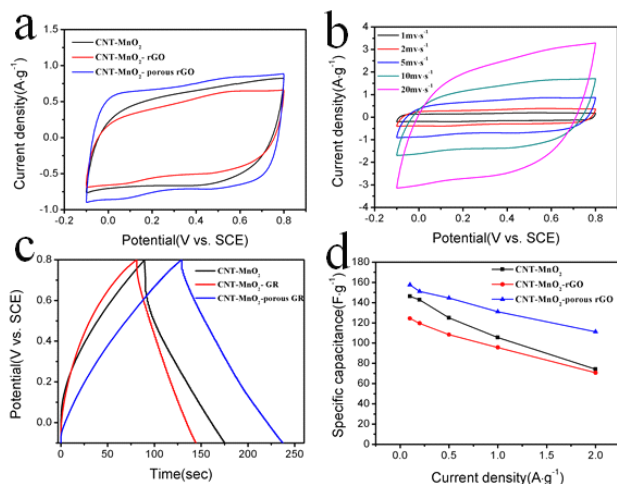


Fig. 5 Electrochemical performance: CV curves comparison of different electrode structures (a) and CV curves of porous rGO wrapped CNT-MnO₂ nanostructures at different scan rates (b); charge/discharge curves (c) and rate performance (d) comparison of different electrode structures.

Fig. 5 shows the electrochemical performance comparison of different electrode structures. Fig. 5a shows cyclic voltammetry (CV) curve comparison of CNT-MnO₂, CNT-MnO₂-rGO and CNT-MnO₂-porous rGO at the scan rate of 5 mV·s⁻¹. It can be seen that the CV curves of CNT-MnO₂-porous rGO show rectangular-like shape relative to the other two samples. The loading of MnO₂ makes CNT-MnO₂ structure brings out pseudocapacitance property. However, CNT-MnO₂-rGO structure has the minimum area, although it shows relatively rectangular. It is because the adsorption of rGO on the surface of CNT-MnO₂ improves the conductivity owing to the contact between two dimensional rGO and MnO₂, but the rGO nanosheets without porous structure obstructs the infiltration of electrolyte into the hierarchical MnO₂ nanostructure, wrinkle rGO tightly wraps the CNT-MnO₂ nanocables as is shown in Fig. 4d, reducing the utilization of MnO₂ and resulting in lower specific capacitance.

From CV curves of CNT-MnO₂-porous rGO, the linear and almost symmetrical curves indicate that the excellent electrochemical reversibility and capacitive performance of this nanocomposite. Meanwhile, the maximum area among the three samples means that the porous rGO nanosheets wrapping improves the electrochemical performance of the electrode. It can be explained that the porous structure could guarantee the wettability of electrolyte for active materials and improve the utilization of MnO₂ for the increased surface conductivity to make a contribution to the electron transportation at the same time. Furthermore, PDDA is a typical water-soluble quaternary ammonium used as conductive electrolytes, and could not be effectively removed in this ternary composite, thus we chose a low concentration of PDDA to prepare their absorption, as a result, the content of PDDA was ultra-low, and thus was not expected to provide significant influence for the electrochemical performance of the ternary composite. Fig. 5b shows that the current response increases gradually with the increase of scan rate. At high scan rates, the CV curves could also keep rectangular and symmetric current-potential shapes, indicating the perfect electrochemical capacitive behavior. Fig. 5c shows the charge/discharge curves of different electrode structures at the current density of 1000 mA·g⁻¹. Compared with the two others, the electrode of CNT-MnO₂-porous rGO has the most symmetrical triangle curves with the longest discharge time and the minimum IR drop of 0.025 V comparing to CNT-MnO₂ nanocables and pristine rGO of 0.100 V and 0.050V respectively (see the enlarged curves of Fig. 5(c) in Fig. S3), owing to the contribution of rGO and porous rGO to the electrical conductivity of the electrodes.^{38,39} It indicates the superior capacitance and good reversibility of this ternary nanocomposite, meaning that the electrode exhibits outstanding charge-discharge with a stable coulombic efficiency, low polarization as well.⁴⁰

Based on the charge-discharge curves, the specific capacitance can be calculated by the formula ($C = I \Delta t / m \Delta V$, where I is the discharge current, Δt is the discharge time, ΔV is the sweeping voltage range, m is the total mass of the electrode material). Fig. 5d shows the calculated capacitance of these electrodes at different current densities, and also exhibits the rate performance. It is clear to see that the CNT-MnO₂ doesn't show very good electrochemical property comparing to the results reported before²⁶, which could be explained that the poor crystalline of δ -MnO₂, which is not the best suitable crystalline of MnO₂ for the application on electrochemical capacitor, affects the electrochemical performance of CNT-MnO₂ and ternary composite based on it to a certain degree.¹² As a comparison, CNT-MnO₂-porous rGO has the best rate performance. The max specific capacitance can achieve 157.6 F·g⁻¹ at a current density of 100 mA·g⁻¹, and even at a current density of 2000 mA·g⁻¹, 111.3 F·g⁻¹ can still be retained, which suggests that about 29% of the specific capacitance is lost when the current density increases from 100 mA·g⁻¹ to 2000 mA·g⁻¹. Though CNT-MnO₂ has higher capacitance than CNT-MnO₂-rGO, the latter (lost about 43%) has better rate performance than the former (lost about 49%). This is

because the absorption of rGO increases the conductivity and facilitates the charge transportation. Compared to CNT-MnO₂-rGO, porous rGO can provide more convenient and faster ion transport. So it easily comes to the conclusion that the rate performance of CNT-MnO₂-porous rGO is superior to CNT-MnO₂ and CNT-MnO₂-rGO.

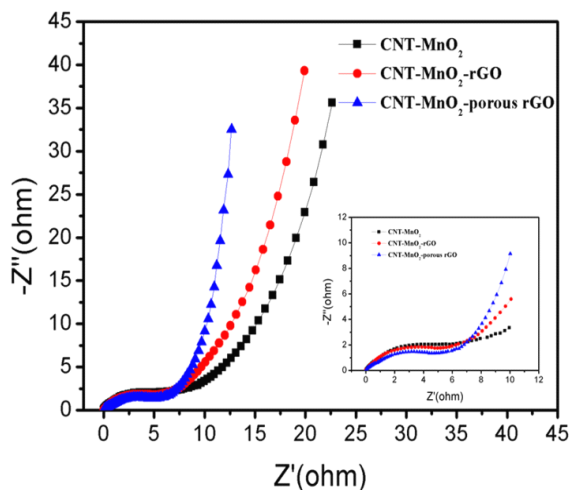


Fig. 6 Nyquist curves comparison of different electrode structures.

The Nyquist plots obtained from electrochemical impedance spectroscopy (EIS) tests are shown in Fig. 6. It is obvious to see that the AC impedance spectra of CNT-MnO₂-porous rGO composed of a depressed arc in the high-frequency region and a straight line in the low-frequency region. The resistance projected by semi-circle is attributed to the electrode materials. Therefore, the ion diffusion resistances of CNT-MnO₂, CNT-MnO₂-rGO and CNT-MnO₂-porous rGO are 8.2, 7.3 and 6.3Ω, respectively.⁴¹ The large Warburg impedance of CNT-MnO₂ should be attributed to both the hydrophobicity and the low conductivity of the electrode surface. The non-porous rGO could improve the conductivity of the electrode, but the ion diffusion issue still existed. As a result, the porous rGO could solve the two problems in a certain extent, thus it has the lowest Warburg impedance. Meanwhile, the low-frequency region of CNT-MnO₂-porous rGO shows a nearly 90° straight line starting from the mid-high frequency, indicating that the CNT-MnO₂-porous rGO nanocomposite is almost purely capacitive in nature⁴² and very suitable to be electrode materials for supercapacitor.

The long-term electrochemical stability was investigated by charge/discharge cycling at the current density of 1000 mA·g⁻¹, as shown in Fig. 7. It can be seen that the specific capacity of CNT-MnO₂-porous rGO can retain 93% after 1000 cycles. It means that this nanocomposite owns a stable electrochemical performance, which profits from the adsorption of porous rGO. It could be also suggested that the flexible property of porous rGO can provide enough cushion space for crystal expansion during the charging/discharging process. The electrochemical performance of the ternary composite in two-electrode system was tested and the results are shown in Fig.S4 in the electronic

supplementary information. It reveals that the specific capacitance of this symmetric supercapacitor could be more than 270 mF·cm⁻². These results mentioned above clearly confirm that the CNT-MnO₂-porous rGO hybrid nanocomposite owns better electrochemical performance with relatively high capacitance and good rate performance which could be derived from the factors as follows. Firstly, the adsorption of porous rGO on the surface of CNT-MnO₂ improves the conductivity of this structure. Secondly, the porous structure makes MnO₂ easier to contact with electrolyte to make use of its pseudocapacitance, and takes full advantage of the double-layer capacitance of rGO at the same time.

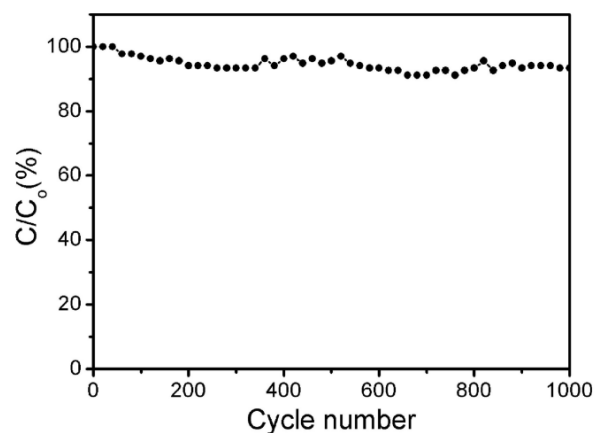


Fig. 7 Cyclic performance of CNT-MnO₂-porous rGO nanostructures at the current density of 1000 mA·g⁻¹.

4. Conclusions

In summary, porous rGO as a superior conductive layer for the electrodes of aqueous supercapacitors has been proved. CNT-MnO₂ nanocables wrapped by porous rGO shows higher specific capacitance and better rate performance than pristine CNT-MnO₂ nanocables and CNT-MnO₂-rGO. It could be attributed to the enhancement of MnO₂ surface conductivity and the convenient contact between electrolyte and MnO₂. Furthermore, the ternary electrode material shows stable cyclic performance. The synthesis strategy has certain effects on the design of good performance electrodes of supercapacitors.

Acknowledgement

We acknowledged the funding support by the National Natural Science Foundation of China (Grant No. 21203238).

Notes and references

^aSuzhou Institute of Nano-tech and Nano-bionics, Chinese Academy of Sciences, Suzhou 215123, P. R. China; Tel: 0512-62872803; E-mail: mhchen2008@sinano.ac.cn (Prof. MH Chen) and qwli2007@sinano.ac.cn (Prof. QW Li)

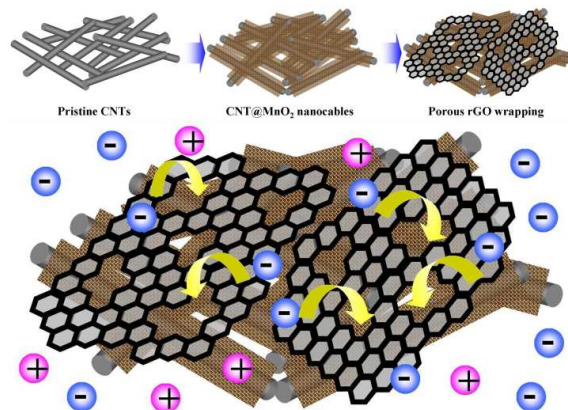
^b School of Material Science and Engineering, Zhengzhou University, Zhengzhou 450001, P. R. China;

^c School of Nano Science and Technology, University of Science and Technology of China, Suzhou, 215123, P. R. China;

^d Zhengzhou Institute of Aeronautical Industry Management, Zhengzhou 450046, P. R. China

1. R. Kořtz and M. Carlen, *Electrochim. Acta*, 2000, 45, 2483-2498.
2. P. Simon and Y. Gogotsi., *Nat. Mater.* 2008, 7, 845-854.
3. G. An, P. Yu and M.J. Xiao, *Nanotechnology*, 2008, 19, 275709-275716.
4. S. B. Ma, K.W. Nam and W.S. Yoon, *J. Power Sources*, 2008, 17, 483-489.
5. F.B. Sillars, S.I. Fletcher and M.Mojtaba, *Energy Environ. Sci.*, 2011, 4, 695-706.
6. J.R. Miller and P. Simon, *Science*, 2008, 321, 651-652.
7. C. Peng, S.W. Zhang and D. Jewell, *Prog. Nat. Sci.*, 2008, 18, 777-788.
8. S.M. Li, Y.S. Wang and S.Y. Yang, *J. Power Sources*, 2013, 225, 347-355.
9. H.L. Wang, H.S. Casalongue, Y.Y. Liang, *J. Am. Chem. Soc.*, 2010, 132, 7472-7477.
10. R.R. Salunkhe, K. Jang and S.W. Lee, *RSC Advances*, 2012, 2, 3190-3193.
11. M. Toupin, T. Brousse and D. Be' langer, *Chem. Mater.*, 2004, 16, 3184-3190.
12. Y. Jin, H.Y. Chen and M.H. Chen, *ACS Appl. Mater. Interfaces*, 2013, 5, 3408-3416.
13. R.H. Baughman, A.A. Zakhidov and W.A. de Heer, *Science*, 2002, 297, 787-792.
14. M.Q. Wu, G.A. Snook and G.Z. Chen, *Electrochem. Commun.*, 2004, 6, 499-504.
15. S.B. Ma, Y.H. Lee and K.Y. Ahn, *J. Electrochem. Soc.*, 2006, 153, 27-32.
16. C.Y. Lee, H.M. Tsai and H.J. Chuang, *J. Electrochem. Soc.*, 2005, 152, 716-720.
17. G.H. Yu, L.B. Hu and N. Liu, *Nano Lett.*, 2011, 11, 4438-4442.
18. Y. Hou, Y.W. Cheng and T. Hobson, *Nano Lett.*, 2010, 10, 2727-2733.
19. L. Nyholm, G. Nyström and A. Mihranyan, *Adv. Mater.*, 2011, 23, 3751-3769.
20. E.J. Yoo, J. Kim, E. Hosono and H.S. Zhou, *Nano Lett.*, 2008, 8, 2277-2282.
21. H.L. Wang, L.F. Cui and Y. Yang, *J. Am. Chem. Soc.* 132 (2010) 13978-13980.
22. L. Li, A.R.O. Raji and J.M. Tour, *Adv. Mater.*, 2013, 25, 375-382.
23. X. Zhao, C.M. Hayner and M.C. Kung, *ACS Nano*, 2011, 5, 8739-8749.
24. X.L. Wang, L.Y. Jiao and K.X. Sheng, *Sci. Rep.*, 2013, 3, 1996.
25. S.B. Ma, K.Y. Ahn and E.S. Lee, *Carbon*, 2007, 45, 375-382.
26. X.B. Jin, W.Z. Zhou and S.W. Zhang, *Small* 2007, 3, 1513-1517.
27. Z.Y. Sun, Z.M. Liu and B.X. Han, *Adv. Mater.*, 2005, 17, 928-932.
28. J. Yan, Z.J. Fan and T. Wei, *J. Power Sources*, 2009, 194, 1202-1207.
29. Y.J. Yang and C.D. Huang, *J. Solid State Electrochem.*, 2010, 14, 1293-1301.
30. S. Devaraj and N. Munichandraiah, *J. Phys. Chem. C*, 2008, 112, 4406-4417.
31. X.F. Xie and L. Gao, *Carbon*, 2007, 45, 2365-2373.
32. C. Julien, M. Massot and R. Baddour-Hadjean, *Solid State Ionics*, 2003, 159, 345-356.
33. C.M. Julien, M. Massot and C. Poinson, *Spectrochim. Acta, Part A*, 2004, 60, 689-700.
34. S.Y. Wang, S.P. Jiang and Xin Wang, *Nanotechnology*, 2008, 19, 265601-265607.
35. J.T. Zhang, J.W. Jiang and X.S. Zhao, *J. Phys. Chem. C*, 2011, 115, 6448-6454.
36. S. Zhang, Y.Y. Shao and H.G. Liao, *ACS Nano*, 2011, 5, 1785-1791.
37. X. Du, X.M. Liu and H.M. Chen, *J. Phys. Chem. C*, 2009, 113, 9063-9070.
38. Z. Bo, W.G. Zhu and W. Ma, *Adv. Mater.*, 2013, 25, 5799-5806.
39. A.L. Najafabadi, T. Yamada and D.N. Futaba, *ACS Nano*, 2011, 5, 811-819.
40. L.H. Bao, J.F. Zang and X.D. Li, *Nano Lett.*, 2011, 11, 1215-1220.
41. J. Bao, C.M. Li and C.X. Guo, *J. Power Sources*, 2008, 180, 676-681.
42. S. Devaraj and N. Munichandraiah, *J. Electrochem. Soc.*, 2007, 1549, 80-88.

Graphical and textual abstract



CNT-MnO₂ wrapped by porous rGO shows improved electrochemical performance owing to the enhanced conductivity and the convenient ion transportation.